Uncovering the nonadiabatic response of geosynchronous electrons to geomagnetic disturbance

J. L. Gannon,[1] S. R. Elkington,[2] and T. G. Onsager[3]

Received 2 February 2012; revised 23 August 2012; accepted 24 August 2012; published 12 October 2012.

[1] We describe an energy spectrum method for scaling electron integral flux, which is measured at a constant energy, to phase space density at a constant value of the first adiabatic invariant which removes much of the variation due to reversible adiabatic effects. Applying this method to nearly a solar cycle (1995–2006) of geosynchronous electron integral flux ($E > 2.0$ MeV) from the GOES satellites, we see that much of the diurnal variation in electron phase space density at constant energy can be removed by the transformation to phase space density at constant μ (4000 MeV/G). This allows us a clearer picture of underlying nonadiabatic electron population changes due to geomagnetic activity. Using scaled phase space density, we calculate the percentage of geomagnetic storms resulting in an increase, decrease, or no change in geosynchronous electrons as 38%, 7%, and 55%, respectively. We also show examples of changes in the electron population that may be different from the unscaled fluxes alone suggest. These examples include sudden electron enhancements during storms which appear during the peak of negative *Dst* for μ-scaled phase space density, contrary to the slow increase seen during the recovery phase for unscaled phase space density for the same event.

Citation: Gannon, J. L., S. R. Elkington, and T. G. Onsager (2012), Uncovering the nonadiabatic response of geosynchronous electrons to geomagnetic disturbance, *J. Geophys. Res.*, *117*, A10215, doi:10.1029/2012JA017543.

1. Introduction

[2] The relative contribution of various energization and loss processes is a topic of continuing debate in radiation belt physics [e.g., *Green and Kivelson*, 2004; *Baker et al.*, 2005]. Radial diffusion is directly affected by the direction and magnitude of the gradient in phase space density [*Li and Temerin*, 2001], and wave-particle interactions may affect the gradient by locally creating particle enhancements and losses [*Meredith et al.*, 2000; *Horne et al.*, 2005]. However, observations of changes in particle fluxes are a complicated superposition of these nonadiabatic processes that directly affect the particle populations themselves, obscured by adiabatic responses to changes in magnetic field geometry and measurement complications as the satellite passes across the drift paths of different populations of particles. By removing adiabatic variation from flux, or phase space density, we can more easily observe changes in the levels of energetic electrons in the Earth's radiation belts due to nonadiabatic effects, including in situ heating and diffusive source and loss processes acting on particle populations in the Earth's magnetosphere.

[3] Magnetic field nonuniformity in the Earth's magnetosphere (gradients in magnitude, field line curvature, topological changes) produces drifts in charged particle trajectories. These drifts define electron dynamics and can also be understood in terms of three adiabatic invariants associated with the three distinct and separable motions that charged particles undergo in the Earth's magnetosphere. These motions are called drift, bounce, and gyromotion, in order of decreasing period. Each of these motions has an associated adiabatic invariant, derived from the action integral [*Goldstein et al.*, 2001]:

First

$$\mu = \frac{p_\perp^2}{2m_o B} \tag{1}$$

Second

$$K = \int \sqrt{B(s)^2 - B_m^2}\, ds \tag{2}$$

Third

$$\phi = \int B \cdot dA \tag{3}$$

The response of a particle to a change that is slower than the invariant's associated motion results in conservation of that invariant. In other words, if the change in the magnetic field of the Earth is slow compared to a particle's gyro, bounce, and drift motion, its energy and location must change in order to

[1]U.S. Geological Survey, Golden, Colorado, USA.
[2]Laboratory for Atmospheric and Space Physics, Boulder, Colorado, USA.
[3]NOAA Space Weather Prediction Center, Boulder, Colorado, USA.

Corresponding author: J. L. Gannon, U.S. Geological Survey, 1711 Illinois St., Golden, CO 80302, USA. (jgannon@usgs.gov)

0148-0227/12/2012JA017543

conserve all three invariants. For example, as the magnetosphere is slowly compressed, an electron must move inward and gain energy in order to conserve its first and second invariants and do the reverse as the magnetosphere relaxes. Energization and loss processes occurring on different time scales will result in the breaking of one or more of these invariants [*Li and Temerin*, 2001; *Meredith et al.*, 2000; *Horne et al.*, 2005]. If we can remove or minimize the impact of adiabatic changes in our analyses, the more interesting nonadiabatic responses will be easier to understand.

[4] Satellites give us information in count rate at a constant energy, typically converted to flux, which reflects particle populations with different adiabatic invariants depending on location and geomagnetic condition. Even in equilibrium conditions of the magnetosphere, as the satellite moves in local time and across field lines, the L^* value changes. As a satellite measures particles of different pitch angle, different values of K are represented. If the magnetic field varies along an orbital trajectory, although the detector energy range is constant, the μ value of measured particles varies.

[5] Phase space density (PSD) is a more physically meaningful measurement than flux because of the constraints of Liouville's theorem, which describes the time evolution of phase space distributions in a volume $d^3\,q d^3\,p$ [*Schulz*, 1996]. The theorem states that the distribution is constant in that volume along any trajectory in phase space and is valid in both equilibrium and nonequilibrium systems. The theorem is stated in coordinate space but can be transformed into a function of the three adiabatic invariants and three phases:

$$f = f(x, y, z, p_x, p_y, p_z; t) => f(\mu, K, L^*, \phi_\mu, \phi_K, \phi_{L^*}; t).$$

In the context of this paper, we average over the action angle variables ϕ_μ, ϕ_K, and ϕ_{L^*} and consider the reduced phase space density, $f = f(\mu, K, L^*)$ [*Schulz*, 1996].

[6] As the magnetic field changes, either as a result of slow variation or movement of the satellite in space, a constant energy detector measures particle flux at varying magnetic moments μ. By transforming to phase space density and removing the adiabatic variation associated with a changing value of μ (due to both changes in field geometry and satellite trajectory), we can remove a layer of complexity from a long time series of particle measurements, allowing a clearer description of the underlying nonadiabatic processes affecting the particle populations themselves. For example, radiation belt particles conserving the third adiabatic invariant will move radially outward in response to those changes in the ring current that lowers the magnetic flux contained within their drift orbit. The result of this so-called RDst effect R is to cause an apparent drop in radiation belt fluxes when measured at constant radial distance and energy, beyond any real losses in the distribution function [e.g., *Kim and Chan*, 1997; *Green and Kivelson*, 2004]. Similarly, drift shell splitting resulting from any noon-midnight asymmetry in the global magnetosphere [e.g., *Roederer*, 1970] will result in flux variations with local time, partly as a result of the global characteristics of the distorted magnetosphere and partly due to variations in the local magnetic field strength [*Onsager et al.*, 2004]. Of particular salience to this effort are the adiabatic variations observed by a geosynchronous detector with a constant energy threshold, which will observe populations with different first adiabatic invariant, μ, as the spacecraft moves across local times into regions of higher or local magnetic field strength. By removing these adiabatic variations in the observed flux and underlying phase space density, we can more easily observe the changes in the radiation belts that result from nonadiabatic processes, including the transport, heating, and loss of radiation belt particles.

2. Method

[7] The geosynchronous electron and magnetic field data used in this analysis are obtained from various GOES satellites (8–12) over 1996 through 2006, which have a time resolution of 5 min and 1 min, respectively. The electron data for the two integral channels (>0.8 MeV and >2.0 MeV) are given as a count rate, which is converted to integral flux using the given instrument geometric factors (0.078 cm^2 sr and 0.05 cm^2 sr, from http://www.swpc.noaa.gov/Data/goes.html). Note that the energy range and geometric factor for the lower-energy channel differ from that given in the original GOES specification but have been updated following a recalibration of the geometric factor [*Hanser*, 2011]. Time periods for which the electron data fall below a threshold count rate (count rate <10, which occurs periodically in the higher-energy channel), or the detector is determined to be outside of the magnetopause, are not used in this analysis.

[8] In order to scale flux measurements to a value independent of adiabatic change, we first calculate phase space density (PSD) from the measured integral flux. Given GOES integral flux, we can calculate PSD at the energy E, according to the method derived by *Onsager et al.* [2004], as follows:

$$f(E) = \frac{c^2 J(>E)}{(E_0^2 + EE_0)2mc^2 + 2E_0^3 + 2EE_0^2 + E^2E_0},$$

where c is the speed of light, m is the mass of the particle, E_0 is the energy spectrum scaling factor, and $J(>E)$ is the integral flux value above the energy in $cm^{-2}\ s^{-1}\ sr^{-1}$, E in MeV, which gives f in $MeV^{-3}\ s^{-3}$. The parameter E_0, the scaling factor of the particle's energy spectrum, is estimated using the two energy channels on the GOES particle detectors by simply fitting these points to an assumed exponential spectrum, as follows:

$$E_0 = (2 - 0.8)/\log(j_{0.8MeV}/(j_{2.0MeV}))$$

To maintain a constant value of the first invariant, a detector would need to vary the energy range of the measurement as the magnetic field strength changes. We transform the constant energy PSD calculated above to PSD with a constant first invariant by applying a scaling factor based on the measured energy spectrum. We use the E_0 factor determined above and the measured magnetic field from GOES to calculate the energy level required to result in the specified μ using its definition and scale PSD as follows (also from *Onsager et al.* [2004]):

$$f(E) = f_0 e^{-E/E_0}$$

We select a value of μ that is near the natural range of values that the electrons being measured would have. This is because the scaling requires an accurate energy spectrum and

the farther away from the measured points, the more likely the spectrum differs from our simple exponential characterization of it. The value we select is 4000 MeV/G for the >2.0 MeV channel.

2.1. Caveats

[9] This method removes the electron flux variation due to the first adiabatic invariant, but the second and third are unaccounted for. The effect of the second invariant is somewhat minimized due to the orientation of the GOES satellite. Because the GOES satellite is three-axis stabilized for the ground-pointing imagers, if the field is fairly stable, the detector is positioned to measure particles with pitch angle around 90°. During relatively quiet conditions, the variation of the central pitch angle is approximately between 85° and 95°, which should impart a relatively small variation on the electron flux. However, during times of large variation in magnetic field orientation at geosynchronous orbit, the relative orientation of the satellite with the field line can vary widely, resulting in particles with a wide range of pitch angles being observed. The effect on the particle flux is most dramatic during storm main phases but may also contribute when the magnetosphere is highly stretched, producing nightside butterfly-type distributions. In addition, the wide field of view of the GOES detector adds uncertainty in the estimation of pitch angle that may impart an additional diurnal signal if there is a local time variation in pitch angle distribution. This uncertainty cannot be resolved in this data set but may be explored in the future, as pitch angle resolved data become available from GOES-13 and beyond.

[10] The third adiabatic invariant is directly related to the L^* value of the measured particle. Because a geosynchronous satellite crosses L shells as it orbits the Earth, if there is a flux gradient in L^*, an additional diurnal variation will be observed in the electron flux time series. However, if the gradient is outward directed at geosynchronous orbit, it should have an opposite effect from the effect of varying μ. As the satellite passes through a smaller L shell on the dayside, a higher flux should be observed than the nightside. The effect of L^* also is an effect due to variations in pitch angle. Let us take an example that assumes the orientation of the satellite is such that it always measures particles of the same pitch angle, just not exactly 90°. If the pitch angle distributions on the dayside are pancake (maximum at 90°) and on the nightside are butterfly (local minimum at 90°), then being slightly off of 90° would yield an apparent decrease in flux on the dayside and increase in flux on the nightside. Due to drift shell splitting, which can occur simply due to field line stretching [*Roederer*, 1970], this situation is really just a restatement of the effect of the third adiabatic invariant, as off-90° particles are at a higher or lower L shell at day or night. Both the variation of L^* with local time and the pitch angle effect due to drift shell splitting only occur in the presence of a gradient in flux with L^*.

[11] If the effect of μ variation in a constant energy detector is effectively removed, the remaining diurnal variation should be due to the smaller effects of the differences in the second and third invariants along an orbital trajectory. An increase in diurnal variation of the μ-scaled PSD after a disturbance may indicate a change in either the radial (L^*) gradient in flux or a change in the pitch angle distribution of the observed particles due to either increase field line stretching or changes in the underlying particle populations.

[12] There are also uncertainties introduced by low count rates observed in the higher-energy channel. If the count rate goes below 10 in that channel, it is considered below threshold and is not used for scaling or calculation of energy spectrum. In this case, an average value of E_0 = 250 keV is used. This value was determined to be a typical one for geosynchronous electron distributions by *Onsager et al.* [2004] and is consistent with values determined from this analysis. However, this analysis is very insensitive to this choice. Other values (E_0 = 150 keV and E_0 = 350 keV) were also tested, and no discernible effect was apparent. The count rate usually only goes below threshold during times of high geomagnetic disturbance when rapidly fluctuating magnetic field lines invalidate the scaling procedure due to variation in pitch angle, as described above.

3. Analysis

3.1. Is the Diurnal Variation Removed?

[13] We first ask if our μ-scaled PSD effectively removes diurnal variation during quiet times due to satellite motion across electron drift shells. The effect of μ scaling should be most noticeable on the daily time scale because of the typical variation in observed magnetic field due to an asymmetric magnetosphere. In Figure 1 the diurnal variation in PSD time series shown for μ-scaled PSD of each example is noticeably flattened and even a bit inverted (which is a radial gradient effect that is discussed later). This suggests that this scaling method accurately removes the adiabatic variation in this period, during which we expect no nonadiabatic changes in the electron population. These measurements are taken from the >2.0 MeV channel and are scaled to μ = 4000 MeV/G. The U.S. Geological Survey (USGS) 1 min *Dst* [*Gannon and Love*, 2011] is also shown as reference for geomagnetic activity (Figure 1c).

3.2. How Do Electrons Respond to Storms? Comparison of Scaled and Unscaled PSD

[14] Scaling electron PSD time series to a constant μ can drastically alter how the particle populations appear to respond to current conditions. The examples in Figure 1 show three time periods in 1997 where the constant μ (μ = 4000 MeV/G) PSD exhibits a different behavior than the constant energy PSD. Figure 1a shows a storm time period in which the trend of the poststorm constant μ time series is generally unchanged, but the constant energy PSD shows a decrease. Because changes in L during the storm complicate the analysis, prestorm and poststorm values must be evaluated well separated from the storm itself. Figure 1b shows the same time period, with the storm blacked out to aid the comparison. The dotted line shows the approximate trend of the prestorm electron PSD in both cases. Other types of PSD differences when using a constant μ adjustment include nonstorm changes being smoothed out (Figure 1c) or storm time enhancements becoming more evident (Figure 1d). Although certainly not all events are changed in one of these ways, differences such as these can have a effect on analyses.

[15] *Reeves et al.* [2003] performed a study of a solar cycle of 1.8–3.5 MeV Polar High-Sensitivity Telescope (HIST) flux levels to analyze the effect of geomagnetic disturbance

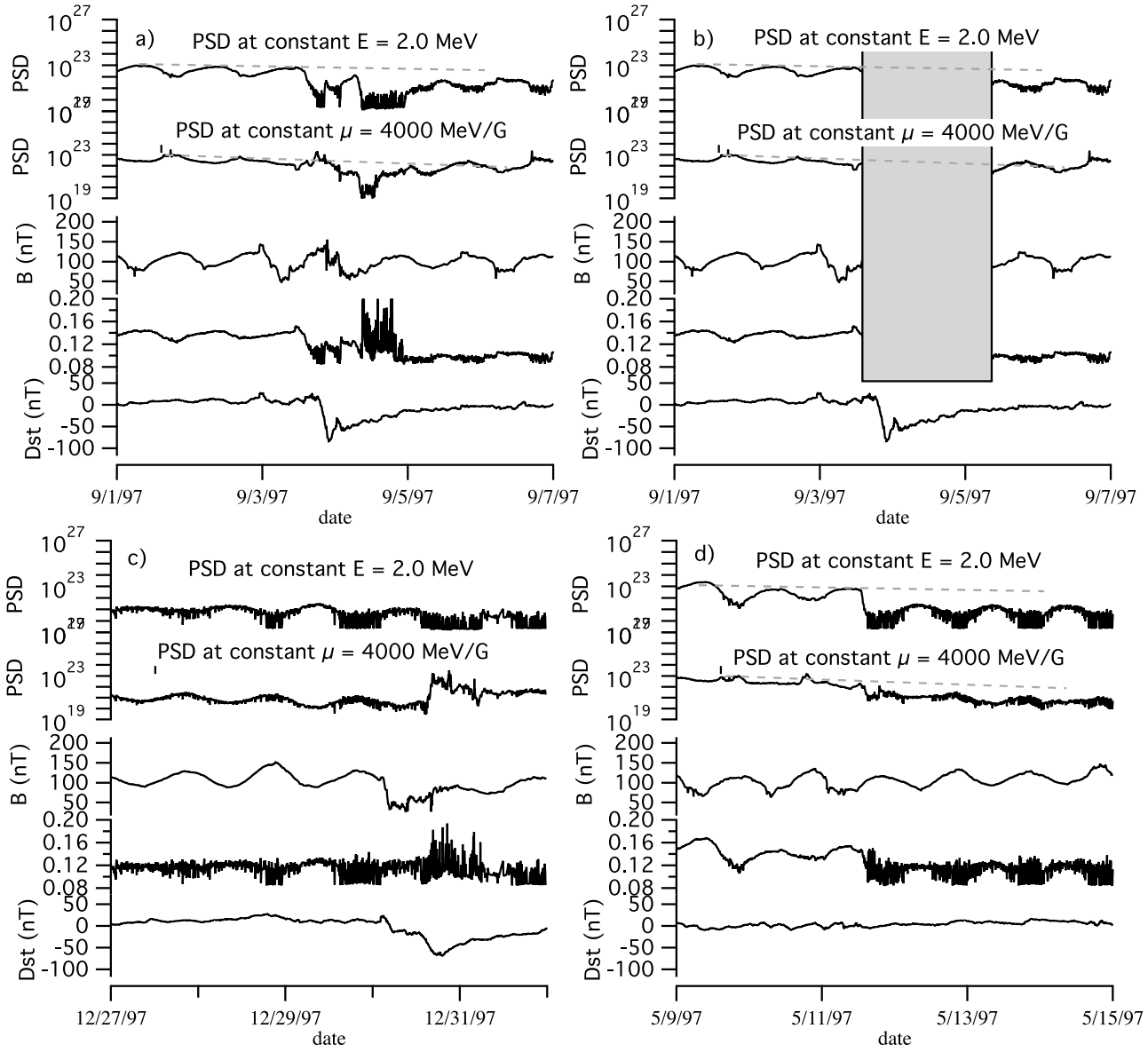

Figure 1. Three storm examples (top curve unscaled (constant energy) PSD; middle curve, μ-scaled (4000 MeV/G) PSD; and bottom curve, USGS *Dst*) showing types of differences seen between constant energy and constant μ PSD time series. (a and b) The same storm period, with the storm itself obscured for μ-scaled for prestorm and poststorm PSD evaluation clarity. (c) A nonstorm example of how constant μ PSD can smooth out sudden observed PSD changes. (d) A storm time example of an enhancement appearing in the constant μ PSD time series.

on geosynchronous electrons. Over their entire data set, they count the number of storms (>50 nT) that produce increases, decreases, and no change in geosynchronous electron flux and find that the occurrences are approximately 53%, 19%, and 28%, respectively. They control adiabatic influences to some degree by considering time periods well before and after the storm.

[16] We apply the same counting rules as the *Reeves et al.* [2003] analysis to the unscaled PSD and μ-scaled PSD in our GOES data set. We have available nearly a solar cycle of similar GOES data, and unlike the Los Alamos National Laboratory satellites, GOES satellites include a magnetometer which allows us to scale to a constant value of μ. There are important differences to note between these data sets: because GOES is geosynchronous, we do not have as wide a range of sampled L values as Reeves et al., who used the Polar HIST data. We cannot even discriminate by L shell, whereas Reeves et al. were able to compare the peak of each enhancement or loss. We can therefore not directly compare with their results. However, we can use these results to see how controlling for adiabatic variation affects our particular results. In contrast with the results of Reeves et al., we find that most of the apparent losses and increases in electron flux become "no change" using scaled PSD.

[17] The results are summarized in Table 1. Because of the somewhat subjective way of determining prestorm and

Table 1. Storms Reaching Minimum |*Dst*| > 50

Change	Constant Energy PSD	Constant μ PSD
Increase	39%	37%
Decrease	28%	7%
No change	32%	55%

Table 2. Storms Reaching Minimum |*Dst*| > 75

Change	Constant Energy PSD	Constant μ PSD
Increase	36%	37%
Decrease	30%	8%
No change	32%	54%

poststorm values, these numbers are simply intended as statement of the possible impact of adiabatic effects on PSD electron time series. Choosing different criteria for comparing prestorm and poststorm values may yield different results. In addition to ignoring the storm itself, it is necessary to minimize the remaining diurnal variation due to PSD gradients in *L* shell by either selecting a single time of day for the comparison or using the average daily PSD value. In this analysis, we use the latter method, illustrated by the dashed lines in Figure 2 (middle). Sporadic short-term variations, data gaps, PSD spikes, and the varying duration of the storm period can lead to unclear situations and misclassification. In this analysis, computer-based classification of the PSD trends was changed for several events based on manual inspection.

[18] The strong prevalence in the μ-scaled PSD is for there to be no change. While the unscaled PSD count does not show the same results as *Reeves et al.* [2003], we do not expect it to, as this is a different time period and the unscaled fluxes are affected by the magnetic field strength at a given time. However, it is important to understand that these apparent statistical changes are due solely to converting the time series to constant μ PSD. In other words, it is possible that a large portion of observed flux variations may actually be due to reversible adiabatic variation, controlled by changing magnetic fields, and analyses attempting to use changes in flux to understand the mechanisms controlling particle variation should be careful to take this into account.

[19] We next separate the storms by *Dst* level (see Tables 2 and 3). This suggests that adiabatic effects can override other effects and should not be ignored in an analysis of electron response or energization mechanism.

3.3. Storm Variations

[20] There appears to be very little change in the scaled PSD statistics with storm strength. We then bin the storms by month of occurrence to examine if there is the seasonal effect on particle populations due to storms is altered by μ scaling. Figure 1 shows how the responses (increase, decrease, or no effect) vary from month to month. An annual signal is seen in the percentages of events causing an increase in scaled electron PSD. The effect is also possibly seen in the unscaled profile, but it is far less clear. This seasonal variation is consistent with the Russell-McPherron effect, which has been shown to strongly control the geoeffectiveness of high-speed streams on relativistic electrons in the radiation belts [*McPherron et al.*, 2008].

3.4. Examples

3.4.1. Main Phase Enhancement

[21] Geomagnetic storm main phases are times of highly varying magnetic field and magnetic field deviation, and

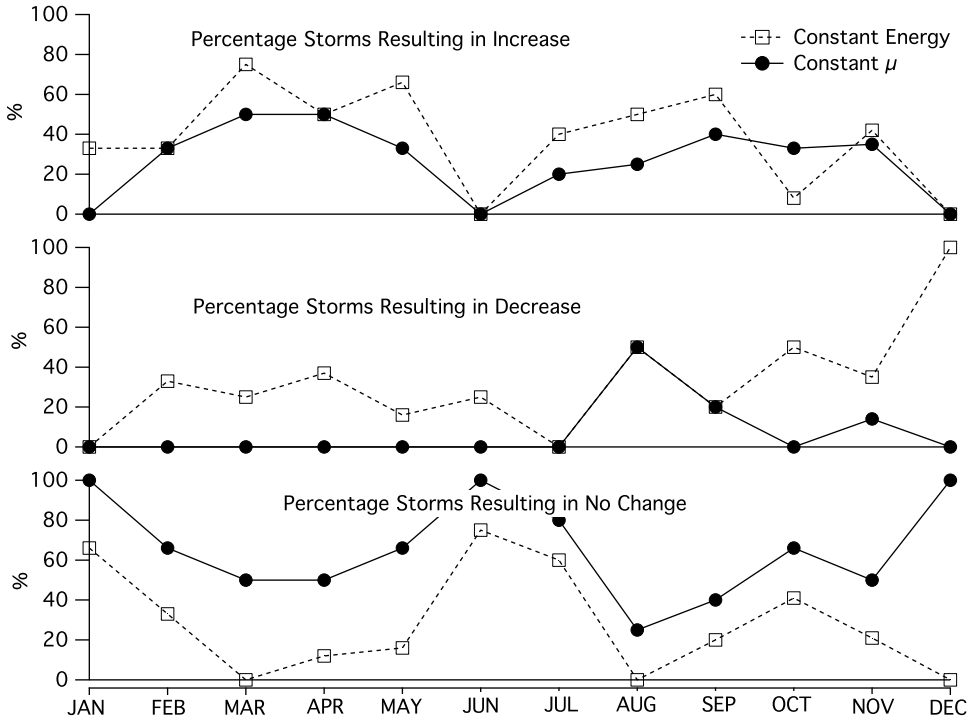

Figure 2. (top) Percentage of storms yielding an increase in geosynchronous electrons versus month. (middle) Percentage of storms yielding a decrease. (bottom) Percentage yielding no change.

Table 3. Storms Reaching Minimum $|Dst| > 100$

Change	Constant Energy PSD	Constant μ PSD
Increase	50%	36%
Decrease	22%	8%
No change	27%	55%

therefore, we may expect electron populations to be greatly affected by adiabatic effects. However, this is also the time that rapidly varying magnetic field direction can invalidate the assumption that we are looking at equatorially mirroring particles and can therefore ignore changes in the second adiabatic invariant. Even with that difficulty, it should be easy to visually identify the short time scale changes due to changing field direction from smoothly varying increases and decreases in the electron population. Figure 3 illustrates a dramatic example of what can be uncovered by removing the effect of the changing magnetic field as it slowly returns to prestorm levels during the storm recovery phase. Instead of the expected gradual increase in electron PSD, we observe a sudden increase just after the peak of negative *Dst.* We cannot determine the exact point of the increase because of the pitch angle affects mentioned, but the change clearly happens on shorter time scales. If this is a picture of the true electron response, unobscured by the adiabatic effects due to a changing magnetic field, the short time scale of the increase could have implications in analyses seeking to determine which energization processes are at work during relativistic flux enhancements.

3.4.2. How Does a Sudden Impulse Affect Electrons?

[22] Sudden impulses, seen as positive jumps in *Dst*, can also result in changes in the geosynchronous electron population. Figure 4 shows an example time period that includes two sudden impulses, separate from any significant additional storm signal or disturbance. The first impulse occurs on day 65 and is accompanied by a gradual loss in scaled PSD (as compared to a sudden loss in unscaled PSD) and a change in the energy spectrum measured by the two GOES energy channels. The second impulse, on day 71, does not occur with a change in energy spectrum, but a change in the character of the PSD time series is observed as the inverted diurnal signal becomes sharper for scaled PSD.

[23] Because L^* and pitch angle effects produce a diurnal variation in flux that is inverted from the μ effect, it is difficult to separate them with this analysis alone. However, an increase in the observed diurnal inversion may indicate an increase in the L^* gradient in flux, as both of the effects are directly dependent on the strength of the gradient. Direct comparison of radial gradient magnitude can only be made during times of equal magnetospheric asymmetry. Because *Dst* shows that the geomagnetic disturbance level is approximately the same before and after the impulse and there is no reason to assume that the observed pitch angle is changing, this increase in the diurnal signal may reflect an increase in the radial gradient in phase space density.

4. Conclusion

[24] Scaling geosynchronous electrons to a constant value of the first invariant, μ, removes much of the reversible adiabatic response of the population to changes in magnetic field. The technique described in this paper effectively removed the μ response to allow a clearer view of the non-adiabatic storm time changes in the electron population. Using μ-scaled PSD from GOES over a solar cycle (1995–2006), we find that the population of relativistic geosynchronous electrons increases, decreases, and remains unchanged after storms 37%, 7%, and 55% of the time,

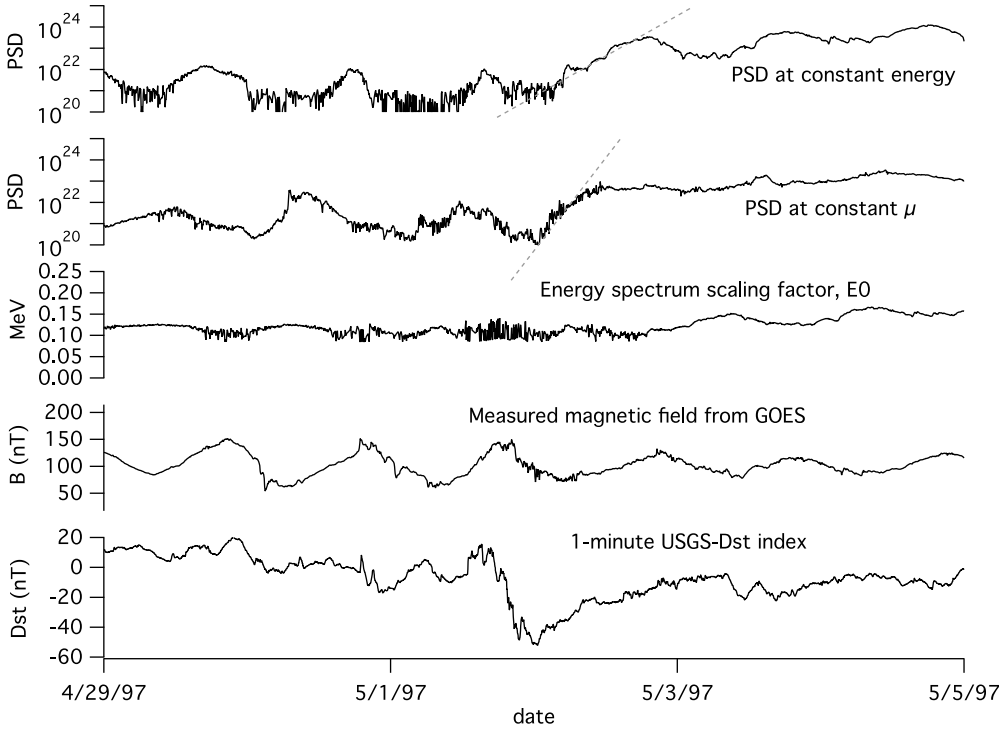

Figure 3. An apparent increase in scaled PSD in the storm main phase.

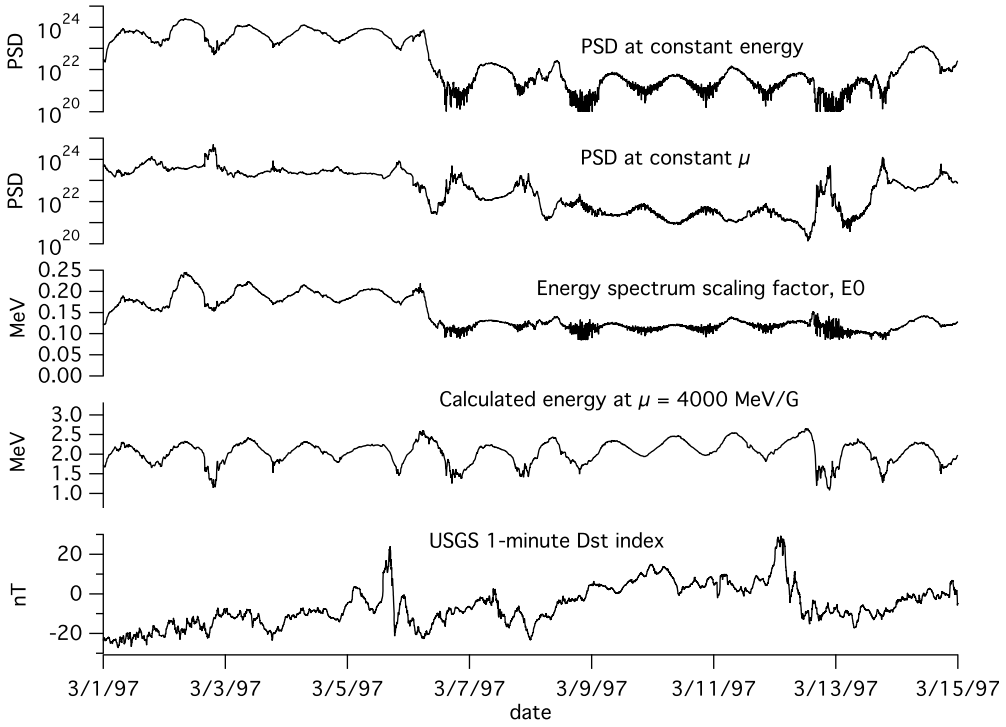

Figure 4. From top to bottom, unscaled (constant energy) PSD; scaled (constant /*mu*) PSD; calculated energy scaling factor; calculated energy at /*mu*=4000 MeV/G; and USGS 1 min *Dst*.

respectively, for storm periods reaching at least −50 nT. These percentages change only slightly when limited to more extreme storm periods.

[25] The removal of adiabatic response from a particle time series can reveal a very different picture of the true response of electrons to geophysical activity. An apparent enhancement or loss may simply be a rearrangement of existing particle populations due to magnetic field reconfiguration or compression. The importance of adiabatic variation in radiation belt electron studies, in particular, should not be underestimated, as revealed by the differences in scaled and unscaled electron PSD shown in this study.

[26] **Acknowledgments.** The authors wish to thank C. A. Finn, J. J. Love and J. V. Rodriguez for reading a draft manuscript. This work was supported by grant NSF-0819963.

[27] Masaki Fujimoto thanks the reviewers for their assistance in evaluating this paper.

References

Baker, D., S. Elkington, X. Li, and M. Wiltberger (2005), Particle acceleration in the inner magnetosphere, in *The Inner Magnetosphere: Physics and Modeling*, *Geophys. Monogr. Ser.*, vol. 155, edited by T. I. Pulkkinen, N. A. Tsyganenko, and R. H. Friedel, pp. 73–85, AGU, Washington, D. C., doi:10.1029/155GM09.

Gannon, J. L., and J. J. Love (2011), One-minute *Dst* index, *J. Atmos. Sol. Terr. Phys.*, *73*, 323–334, doi:10.1016/j.jastp.2010.02.013.

Goldstein, H., C. P. Poole, and J. L. Safko (2001), *Classical Mechanics*, 3rd ed., Addison-Wesley, Reading, Mass.

Green, J. C., and M. G. Kivelson (2004), Relativistic electrons in the outer radiation belt: Differentiating between acceleration mechanisms, *J. Geophys. Res.*, *109*, A03213, doi:10.1029/2003JA010153.

Hanser, F. A. (2011), EPS/HEPAD calibration and data handbook, *Tech. Rep. GOESN-ENG-048D*, Assurance Technol. Corp., Carlisle, Mass.

Horne, R. B., R. M. Thorne, S. A. Glauert, J. M. Albert, N. P. Meredith, and R. R. Anderson (2005), Timescale for radiation belt electron acceleration by whistler mode chorus waves, *J. Geophys. Res.*, *110*, A03225, doi:10.1029/2004JA010811.

Kim, H.-J., and A. A. Chan (1997), Fully-adiabatic changes in storm-time relativistic electron fluxes, *J. Geophys. Res.*, *102*, 22,107–22,116.

Li, X., and M. A. Temerin (2001), The electron radiation belt, *Space Sci. Rev.*, *95*(1–2), 569–580, doi:10.1023/A:1005221108016.

McPherron, R. L., D. N. Baker, and N. U. Crooker (2008), Role of the Russell-McPherron effect in the acceleration of relativistic electrons, *J. Atmos. Sol. Terr. Phys.*, *71*, 1032–1044, doi:10.1016/j.jastp.2008.11.002.

Meredith, N., R. Horne, A. Johnstone, and R. Anderson (2000), The temporal evolution of electron distributions and associated wave activity following substorm injections in the inner magnetosphere, *J. Geophys. Res.*, *105*, 12,907–12,917.

Onsager, T. G., A. A. Chan, Y. Fei, S. R. Elkington, J. C. Green, and H. J. Singer (2004), The radial gradient of relativistic electrons at geosynchronous orbit, *J. Geophys. Res.*, *109*, A05221, doi:10.1029/2003JA010368.

Reeves, G. D., K. L. McAdams, R. H. W. Friedel, and T. P. O'Brien (2003), Acceleration and loss of relativistic electrons during geomagnetic storms, *Geophys. Res. Lett.*, *30*(10), 1529, doi:10.1029/2002GL016513.

Roederer, J. G. (1970), *Dynamics of Geomagnetically Trapped Radiation*, Springer, New York.

Schulz, M. (1996), Canonical coordinates for radiation-belt modeling, in *Radiation Belts: Models and Standards*, *Geophys. Monogr. Ser.*, vol. 97, edited by J. F. Lemaire, D. Heynderickx, and D. N. Baker, pp. 153–160, AGU, Washington, D. C., doi:10.1029/GM097p0153.